Transmission zero in a quantum dot with strong electron-electron interaction: Perturbative conductance calculations

Sejoong Kim and Hyun-Woo Lee
Department of Physics, Pohang University of Science and Technology, Pohang, Kyungbuk 790-784, Korea
(Dated: February 6, 2008)

A pioneering experiment [E. Schuster, E. Buks, M. Heiblum, D. Mahalu, V. Umansky, and Hadas Shtrikman, Nature (London) **385**, 417 (1997)] reported the measurement of the transmission phase of an electron traversing a quantum dot and found the intriguing feature of a sudden phase drop in the conductance valleys. Based on the Friedel sum rule for a spinless effective one-dimensional system, it has been previously argued [H.-W. Lee, Phys. Rev. Lett. **82**, 2358 (1999)] that the sudden phase drop should be accompanied by the vanishing of the transmission amplitude, or transmission zero. Here we address roles of strong electron-electron interactions on the electron transport through a two-level quantum dot where one level couples with the leads much more strongly than the other level does [P. G. Silvestrov and Y. Imry, Phys. Rev. Let. **85**, 2565 (2000)]. We perform a perturbative conductance calculation with an explicit account of large charging energy and verify that the resulting conductance exhibits the transmission zero, in agreement with the analysis based on the Friedel sum rule.

PACS numbers: Valid PACS appear here

I. INTRODUCTION

A pioneering experiment [1, 2] on an Aharonov-Bohm ring containing a quantum dot reported the measurement of magnetic-flux-dependent interference signals and extracted the phase of the transmission amplitude of an electron traversing a quantum dot. The transmission phase rises by π as a new electron is introduced to the quantum dot and the measured phase profile [2] near the Coulomb blockade resonance is in agreement with the Breit-Wigner formula [3]. The experiment revealed at the same time rather strange behaviors of the transmission phase; the transmission phase drops by π almost suddenly in many conductance valleys and the transmission phase behaviors near two neighboring resonance peaks are the same (up to 2π) instead of showing a relative shift by π. The sudden phase drop and in-phase resonances were later reproduced in other experiments [4]. Recently it was reported [5] that similar features persist in quantum dots with a relatively small number of electrons $\gtrsim 10$. The experimental report [1, 2] induced a considerable amount of theoretical investigations [6, 7, 8, 9, 10, 11, 12].

It is well known that the behavior of the transmission phase is constrained by the Friedel sum rule [13] that relates the determinant of the scattering matrix with the number of electrons in the system. The constraint becomes especially severe in one-dimensional systems and reduces to the form $\Delta Q/e = \Delta\arg(t)/\pi$ in strictly one-dimensional systems without any transverse degrees of freedom and without any side branches. Here Q is the total charge in a system, t is the transmission amplitude, and $\arg(t)$ represents the phase of t. Since ΔQ rises by e near each resonance peak but does not change in the conductance valleys, the strictly one-dimensional form of the Friedel sum rule predicts that the transmission phase rises by π only near each resonance. Thus in this prediction, a sudden phase drop in the conductance valleys is not possible and the transmission phase behaviors near two neighboring resonance peaks should differ by π. Therefore the experimental results in Ref. [2] are not compatible with the strictly one-dimensional form of the Friedel sum rule.

Shortly after the experimental report [2], three theoretical calculations [9, 10, 11] on the transport through a two-dimensional quantum dot or a quantum dot with a side branch were reported. It is found that when the quantum dot is linked to external electrodes via quantum point contacts so that a transport through the quantum dot becomes effectively one-dimensional, the transmission phase does not follow the predictions of the strictly one-dimensional form of the Friedel sum rule and does show the sudden phase drops and in-phase resonances in close agreement with the experimental results [2]. Interestingly the transmission amplitude is found to vanish (within the accuracy of the numerical calculation) whenever the sudden phase drop occurs. The calculation results are interpreted in terms of the Fano resonance [14], which can occur when the electron transport process mediated by a level, which is weakly coupled to the electrodes, interferes with the electron transport process mediated by a level, which is relatively strongly coupled to the electrodes. We remark that such fluctuations of the coupling strength require some deviations from strict one-dimensionality and are not possible in strictly one-dimensional systems. The Fano-resonance-based theory of the experimental results is further examined in the recent literatures [15, 16]. Unfortunately the electron-electron interaction effect is largely ignored in the Fano-resonance-based theory. Experimentally the appearance of the Fano resonance and its relation with the in-phase resonances were addressed in a quantum-dot-embedded Aharonov-Bohm interferometer [17].

One of us [8] examined the implications of the Friedel

sum rule in spinless *effectively* one-dimensional systems with time-reversal symmetry. It is found that the general Friedel sum rule $\Delta Q/e = [\Delta \ln \mathrm{Det}(\mathbf{S})]/2\pi i$, where $\mathbf{S}$ is the 2×2 scattering matrix [18], does *not* reduce to the strictly one-dimensional form since $\Delta \ln \mathrm{Det}(\mathbf{S})/2i$ can differ from $\Delta \arg(t)$ by π whenever the transmission amplitude vanishes identically (transmission zero). Similar conclusions are obtained in Ref. [19]. Thus the experimental results in Ref. [2] do not violate the Friedel sum rule as long as the sudden phase drop is accompanied by transmission zero [20]. Moreover it is argued [8] based on the Friedel sum rule that the transmission zero is rather generic and robust in effectively one-dimensional systems since it is related to the topological structure [21] of the Friedel sum rule.

Silvestrov and Imry [12] reported interesting effects of the strong electron-electron interaction on the transport through a quantum dot that is in the intermediate regime between integral and fully chaotic. They found that in such a semichaotic regime, certain single-particle levels in the quantum dot couple strongly with the leads while other levels couple very weakly with the leads [22]. Thus in such a semichaotic quantum dot, the widths of single-particle levels can differ from each other by orders of magnitude and in this sense, the situation addressed by Silvestrov and Imry is similar to that assumed for the Fano-resonance-based theory [9, 10, 11]. But differently from the Fano-resonance-based theory, they focused on the roles of the electron-electron interaction. In the strong interaction (or large charging energy) limit, they found that a new electron introduced to a quantum dot at a resonance peak may occupy a broad level with *higher* bare single-particle energy rather than narrow levels with lower bare single-particle energy, provided that the energy gain via the hopping-induced downward level shift for the broad level can overcome the bare single-particle spacing. It was also found that as the gate voltage is increased towards the next Coulomb blockade peak, the energy gain disappears in the conductance valley between the two consecutive peaks and the electron in the broad level is transferred to an empty narrow level with lower bare single-particle energy. It was noted that the population switching of the broad level can be repeated over many consecutive resonance peaks, providing a natural explanation for the in-phase resonances. It was also argued that the electron transfer from the broad level to a narrow level is responsible for the sudden phase drop. Thus the interaction-based theory of Silvestrov and Imry also produces a phase behavior in close resemblance with the experimental results [2].

In this paper, we revisit the population switching problem addressed by Silvestrov and Imry [12]. We focus on the gate voltage region in the conductance valleys where the transmission phase drops suddenly by π due to the electron transfer from the broad level to a narrow level. Our study is motivated by the observation that while the analysis [8] based on the Friedel sum rule predicts the sudden phase drop to be accompanied by a transmission zero and the prediction is indeed satisfied in the Fano-resonance-based theory [9, 10, 11, 15], the relation between the sudden phase drop and the transmission zero is not clear in the interaction-based theory. Reference [12] is rather focused on the equilibrium ground state configuration and does not address the transport properties in detail. A later publication [23] addressed the conductance behavior near the gate voltage range where the electron transfer occurs from the broad level to narrow levels. However it is rather focused on roles of the spin degrees of freedom and the relation between the sudden phase drop and the transmission zero is not addressed. Recalling that the Friedel sum rule [13] remains valid even in the presence of the electron-electron interaction [24] and that the transmission zero is an essential feature for the sudden phase drop to be compatible with the Friedel sum rule (at least when spin degrees of freedom are not important), the relation between the sudden phase drop and the transmission zero in the interaction-based theory needs clarification. The goal of this paper is to verify this relation in the presence of the strong electron-electron interaction.

The paper is organized as follows. The model Hamiltonian and calculations of equilibrium and transport properties are given in Sec. II. The results are discussed in Sec. III.

II. MODEL AND CALCULATION

For calculation, we use the following model Hamiltonian,

$$H = H_{\mathrm{dot}} + H_{\mathrm{int}} + H_{\mathrm{lead}} + H_t, \tag{1}$$

where

$$\begin{aligned}
H_{\mathrm{dot}} &\equiv \varepsilon_1 c_1^\dagger c_1 + \varepsilon_N c_N^\dagger c_N, && (2)\\
H_{\mathrm{int}} &\equiv U_{\mathrm{CB}} c_1^\dagger c_1 c_N^\dagger c_N, && (3)\\
H_{\mathrm{lead}} &\equiv \sum_k \varepsilon(k) a_k^\dagger a_k + \sum_l \varepsilon(l) b_l^\dagger b_l, && (4)\\
H_t &\equiv \sum_k \left(t_1^{(\mathrm{L})} c_1^\dagger a_k + t_N^{(\mathrm{L})} c_N^\dagger a_k + H.c. \right) && (5)\\
&\quad + \sum_l \left(t_1^{(\mathrm{R})} c_1^\dagger b_l + t_N^{(\mathrm{R})} c_N^\dagger b_l + H.c. \right),
\end{aligned}$$

where a_k, b_l, and c_i $(i = 1, N)$ denote the electron annihilation operators for electrons in the left and right electrodes and in the quantum dot, respectively. U_{CB} is the constant charging energy due to electron interaction in a quantum dot. $t_i^{(j)}$ is a hopping coefficient of electrons moving from the lead j (L for the left lead and R for the right lead) to the dot state i. In order to make the model as simple as possible while keeping the main physics of the broad level population switching in a semichaotic dot, the quantum dot is assumed to have only two single-particle levels (levels $i = 1$ and $i = N$),

where one of them (level N) is a broad level with larger couplings with the leads and the other (level 1) is a narrow level with smaller couplings with the leads. ε_1 and ε_N denote single-particle energies of dot states $|1\rangle$ and $|N\rangle$, respectively, which can be modulated by the gate voltage V_g,

$$\varepsilon_i(V_g) = \varepsilon_i(0) - \kappa e V_g, \tag{6}$$

where $-e(<0)$ is the electron charge and κ is a dimensionless constant depending on the gate geometry. $\varepsilon(k)$, the energy of an electron in the leads, is defined as

$$\varepsilon(k) = \frac{\hbar^2 k^2}{2m} - \epsilon_F, \tag{7}$$

where ϵ_F is the Fermi energy. Note that the one-dimensional dispersion relation is assumed for the leads in order to describe a quantum dot coupled to external electrodes via quantum point contacts. We are interested in temperature regimes well above the Kondo temperature and for simplicity, electron spin degrees of freedom are ignored. This model is the exactly same as the model Hamiltonian analyzed in Ref. [12] except for a trivial generalization from a single lead to two leads. Below electron transport from one lead to the other lead via the quantum dot will be investigated.

Reference [12] addressed the situation (though only one lead is taken into account) where the broad level lies above the narrow level ($\varepsilon_N > \varepsilon_1$). By using the nondegenerate perturbation theory with $H_{\rm dot} + H_{\rm int} + H_{\rm lead}$ as an unperturbed part and H_t as a perturbation, it was noted that the large second order energy correction ($\propto |t_N|^2$) for the broad level can be larger than the bare energy level splitting $\varepsilon_N - \varepsilon_1$ in the semichaotic dot. After careful comparison of the two possible configuration of the dot state in the gate voltage range where only one electron is allowed in the dot, it was concluded that it is energetically favorable for an electron in the dot to occupy the broad level in the lower half of the gate voltage range and to occupy the narrow level in the upper half of the gate voltage range. In the next two subsections, we first reexamine the problem of the ground configuration in the gate voltage range where the electron transfer occurs from the broad level to the narrow level.

A. Effective Hamiltonian

In order to systematically address the gate voltage range very close to the electron transfer, where the bare energy level spacing $\varepsilon_N - \varepsilon_1$ competes with the second order energy correction via hopping, an equal footing treatment of the two competing energy scales is desired. For this purpose, we derive in this subsection an effective Hamiltonian that facilitates such an equal footing treatment. Recalling that the electron number fluctuation in the dot is strongly suppressed in the conductance valley under investigation, one can construct an effective Hamiltonian that acts only on a special subspace of states with a single electron in the dot. For a given energy eigenket $|\Psi\rangle$ of H with $H|\Psi\rangle = E|\Psi\rangle$, its projection $P_1|\Psi\rangle$ onto the subspace with only one electron in the dot becomes an energy eigenket of $H_{\rm eff}$,

$$H_{\rm eff} = H_{11} + H_{10}\frac{1}{E - H_{00}}H_{01} + H_{12}\frac{1}{E - H_{22}}H_{21}, \tag{8}$$

where $H_{mn} = P_m H P_n$ and P_n is a projection operator onto the subspace of states with n electrons in the dot. Equation (8) can be derived by using the Schrieffer-Wolff transformation [25]. Note that the resulting Schrödinger equation $H_{\rm eff}\left[P_1|\Psi\rangle\right] = E\left[P_1|\Psi\rangle\right]$ is a self-consistency equation in the sense that $H_{\rm eff}$ itself contains the exact energy eigenvalue E. As long as the exact E is used, the transformation from H to $H_{\rm eff}$ is exact.

Next we apply the perturbation theory to $H_{\rm eff}$. We decompose $H_{\rm eff}$ into the unperturbed Hamiltonian $H_{\rm unpert}$ and the perturbation H' as follows:

$$\begin{aligned} H_{\rm eff} &= H_{\rm unpert} + H^{'}, \\ H_{\rm unpert} &= P_1\left[\varepsilon_{\rm ave}\left(c_1^\dagger c_1 + c_N^\dagger c_N\right)\right]P_1 \\ &\quad + P_1\left[H_{int} + H_{lead}\right]P_1, \\ H^{'} &= P_1\left[\frac{\varepsilon_1 - \varepsilon_N}{2}\left(c_1^\dagger c_1 - c_N^\dagger c_N\right)\right]P_1 \\ &\quad + H_{10}\frac{1}{E - H_{00}}H_{01} + H_{12}\frac{1}{E - H_{22}}H_{21}, \end{aligned} \tag{9}$$

where $\varepsilon_{\rm ave} \equiv (\varepsilon_1 + \varepsilon_N)/2$. Note that $H_{\rm dot}$ is split into two parts, the average energy part (the first term in $H_{\rm unpert}$ proportional to $\varepsilon_{\rm ave}$) and the level spacing part (the first term in H' proportional to $\varepsilon_N - \varepsilon_1$). Since the level spacing part is included in H' together with the last two terms of H', which are of order t^2 and responsible for the energy correction by hopping, the perturbation calculation with H' as a perturbation provides a desired equal footing treatment of the two competing energy scales. For the purpose of the first order perturbation in H', E in H' may be replaced by $E^{(0)}$ (unperturbed energy eigenvalue of $H_{\rm unpert}$) since the difference $E - E^{(0)}$ affects only higher order perturbation calculations.

B. Ground state

Unperturbed ground states of $H_{\rm unpert}$ are doubly degenerate and given by

$$\begin{aligned} |\varphi_1\rangle &= c_1^\dagger|{\rm vacuum}\rangle, \\ |\varphi_N\rangle &= c_N^\dagger|{\rm vacuum}\rangle, \end{aligned}$$

where $|{\rm vacuum}\rangle$ is defined as the state with zero electron in the dot and single-particle-levels in the leads completely filled up to the Fermi level. The corresponding unperturbed ground state eigenenergy is $E_0^{(0)} = \varepsilon_{\rm ave} + \sum_{k<k_F}\varepsilon(k) + \sum_{l<k_F}\varepsilon(l)$. The degeneracy is lifted by the perturbation H'. According to the degenerate perturbation theory, the first-order energy corrections are

eigenvalues of H' within the subspace spanned by $|\varphi_1\rangle$ and $|\varphi_N\rangle$:

$$\begin{pmatrix} \langle H'\rangle_{11} & \langle H'\rangle_{1N} \\ \langle H'\rangle_{N1} & \langle H'\rangle_{NN} \end{pmatrix} = \begin{pmatrix} \langle\varphi_1|H'\left(E=E_0^{(0)}\right)|\varphi_1\rangle & \langle\varphi_1|H'\left(E=E_0^{(0)}\right)|\varphi_N\rangle \\ \langle\varphi_N|H'\left(E=E_0^{(0)}\right)|\varphi_1\rangle & \langle\varphi_N|H'\left(E=E_0^{(0)}\right)|\varphi_N\rangle \end{pmatrix}, \tag{10}$$

where

$$\begin{aligned}
\langle H'\rangle_{11} =& \frac{\varepsilon_1-\varepsilon_N}{2} - \frac{\Gamma_1^{(\mathrm{L})}+\Gamma_1^{(\mathrm{R})}}{2\pi}\ln\frac{4\epsilon_F}{|\varepsilon_{\mathrm{ave}}|} \\
& - \frac{\Gamma_N^{(\mathrm{L})}+\Gamma_N^{(\mathrm{R})}}{2\pi}\ln\frac{4\epsilon_F}{\varepsilon_{\mathrm{ave}}+U_{\mathrm{CB}}}, \\
\langle H'\rangle_{1N} =& -\frac{1}{2\pi}\left(\sqrt{\Gamma_1^{(\mathrm{L})}\Gamma_N^{(\mathrm{L})}}e^{-i\Delta\theta^{(\mathrm{L})}} + \sqrt{\Gamma_1^{(\mathrm{R})}\Gamma_N^{(\mathrm{R})}}e^{-i\Delta\theta^{(\mathrm{R})}}\right) \\
& \times\left(\ln\frac{\varepsilon_{\mathrm{ave}}+U_{\mathrm{CB}}}{|\varepsilon_{\mathrm{ave}}|}\right), \\
\langle H'\rangle_{N1} =& -\frac{1}{2\pi}\left(\sqrt{\Gamma_1^{(\mathrm{L})}\Gamma_N^{(\mathrm{L})}}e^{i\Delta\theta^{(\mathrm{L})}} + \sqrt{\Gamma_1^{(\mathrm{R})}\Gamma_N^{(\mathrm{R})}}e^{i\Delta\theta^{(\mathrm{R})}}\right) \\
& \times\left(\ln\frac{\varepsilon_{\mathrm{ave}}+U_{\mathrm{CB}}}{|\varepsilon_{\mathrm{ave}}|}\right), \\
\langle H'\rangle_{NN} =& \frac{\varepsilon_N-\varepsilon_1}{2} - \frac{\Gamma_N^{(\mathrm{L})}+\Gamma_N^{(\mathrm{R})}}{2\pi}\ln\frac{4\epsilon_F}{|\varepsilon_{\mathrm{ave}}|} \\
& - \frac{\Gamma_1^{(\mathrm{L})}+\Gamma_1^{(\mathrm{R})}}{2\pi}\ln\frac{4\epsilon_F}{\varepsilon_{\mathrm{ave}}+U_{\mathrm{CB}}}.
\end{aligned}$$

Here $\Gamma_1^{(\mathrm{L})} \equiv 2\pi\left|t_1^{(\mathrm{L})}\right|^2\frac{dn}{d\varepsilon(k)}|_{\varepsilon(k)=0}$, and $\Delta\theta^{(\mathrm{L})} \equiv \arg(t_N^{(\mathrm{L})}) - \arg(t_1^{(\mathrm{L})})$. $\Delta\theta^{(\mathrm{R})}$, $\Gamma_1^{(\mathrm{R})}$, $\Gamma_N^{(\mathrm{L})}$, and $\Gamma_N^{(\mathrm{R})}$ are defined in a similar way. The correct zeroth-order ground state $|\psi_0^{(0)}\rangle = \alpha|\varphi_1\rangle + \beta|\varphi_N\rangle$ is also determined by Eq. (10) since $\binom{\alpha}{\beta}$ is a normalized eigenvector that corresponds to the lower eigenvalue of Eq. (10). Note that when the off-diagonal matrix elements of Eq. (10) are ignored, the eigenvectors are $\binom{1}{0}$ and $\binom{0}{1}$ and the first order energy corrections, which are the diagonal matrix elements of Eq. (10), reproduce the result in Ref. [12] except for trivial corrections due to the extension from a single lead to two leads. The dashed lines in Fig. 1(a) depict the energy eigenvalues of Eq. (10) without the off-diagonal matrix elements. Note that two levels cross at a certain gate voltage, at which the electron configuration changes suddenly from $\binom{0}{1}$ to $\binom{1}{0}$. The inclusion of the off-diagonal matrix elements modifies the result near the level crossing point. As Fig. 1(a) shows, the level crossing is avoided (solid line), and the configuration change of the dot level occurs smoothly over a finite gate voltage range [Fig. 1(b)]. Later it turns out that the deviation of the eigenvector $\binom{\alpha}{\beta}$ from $\binom{1}{0}$ and $\binom{0}{1}$ near the avoided crossing is important for the relationship between the sudden phase drop and the transmission zero. A similar avoided crossing is reported in Ref. [23] which addresses roles of the spin degrees of freedom [26].

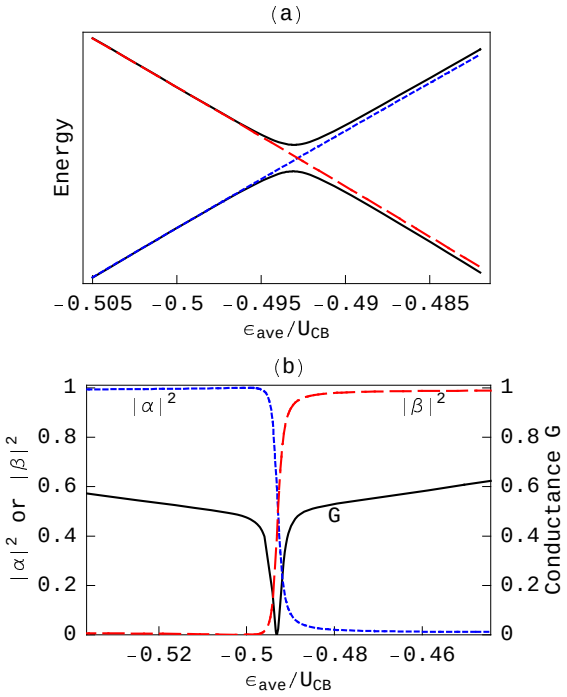

FIG. 1: (Color online) (a) Energy eigenvalues of Eq. (10) as a function of $\varepsilon_{\mathrm{ave}}/U_{\mathrm{CB}}$. When the off-diagonal matrix elements are ignored, two energy levels cross (blue short-dashed line and red long-dashed line). When off-diagonal matrix elements are taken into account, the energy level crossing is avoided (solid lines). (b) $|\alpha|^2$ (blue short-dashed line) and $|\beta|^2$ (red long-dashed line) as a function of $\varepsilon_{\mathrm{ave}}/U_{\mathrm{CB}}$, where $\binom{\alpha}{\beta}$ and $\binom{\beta^*}{-\alpha^*}$ are two eigenvectors of Eq. (10) corresponding to lower and higher energy eigenvalues shown in (a). Conductance (black solid line) is also shown. The conductance is multiplied by a proper factor to fit in the graph box. Thus the marked conductance values are in arbitrary units. Note that the conductance shows a dip near the avoided crossing. In this plot, the time reversal symmetry is assumed and the conductance becomes zero (transmission zero) at the center of the dip. Here $t_1^{(\mathrm{L})}/t_1^{(\mathrm{R})} = 1$, $t_N^{(\mathrm{L})}/t_1^{(\mathrm{R})} = 10$, $t_N^{(\mathrm{R})}/t_1^{(\mathrm{R})} = 11$.

C. Conductance

A standard linear response calculation in the Appendix A results in the following formula for the linear response conductance,

$$G = \frac{\pi e^2}{4\hbar}\lim_{\omega\to 0^+}\left[\mathcal{N}\left(E_0+\hbar\omega\right)\hbar\omega\right]\overline{\left|\langle\Psi_0|\delta\hat{N}^{\mathrm{diff}}|\Psi_n\rangle\right|^2}_{E_n=E_0+\hbar\omega}, \tag{11}$$

where $\mathcal{N}(E)$ is the many-body density of states, $|\Psi_n\rangle$ is the n-th excited states of H with energy E_n, $\delta\hat{N}^{\mathrm{diff}} \equiv \hat{N}^{\mathrm{diff}} - \langle\Psi_0|\hat{N}^{\mathrm{diff}}|\Psi_0\rangle$, $\hat{N}^{\mathrm{diff}} \equiv \sum_k a_k^\dagger a_k - \sum_k b_k^\dagger b_k$,

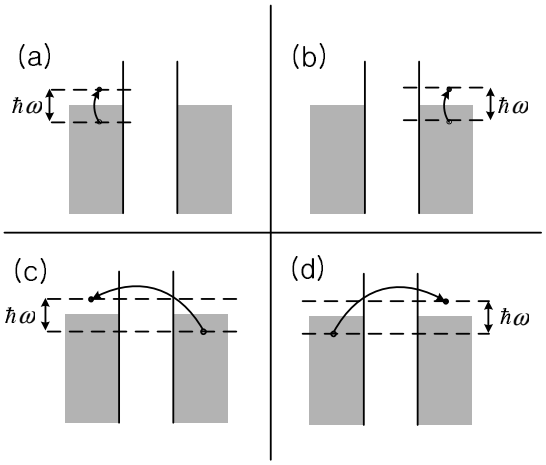

FIG. 2: Schematic plots of four groups of excited states $|\Psi_n\rangle$ that contain an electron-hole pair excitation in the leads with the excitation energy $\hbar\omega$.

and $\overline{\left|\langle\Psi_0|\delta\hat{N}^{\rm diff}|\Psi_n\rangle\right|^2}_{E_n=E_0+\hbar\omega}$ represents the average of $\left|\langle\Psi_0|\delta\hat{N}^{\rm diff}|\Psi_n\rangle\right|^2_{E_n=E_0+\hbar\omega}$ over states $|\Psi_n\rangle$ with $E_n = E_0+\hbar\omega$. Note that Eq. (11) is expressed in terms of the energy eigenstates and eigenvalues of the original Hamiltonian H.

In the limit $\omega \to 0^+$, $\mathcal{N}(E_0+\hbar\omega)$ and $\overline{\left|\langle\Psi_0|\delta\hat{N}^{\rm diff}|\Psi_n\rangle\right|^2}_{E_n=E_0+\hbar\omega}$ for the original Hamiltonian H can be evaluated by using the effective Hamiltonian $H_{\rm eff}$. Here we evaluate Eq. (11) up to the second order in Γ and $\varepsilon_N-\varepsilon_1$. We first evaluate $\mathcal{N}(E_0+\hbar\omega)$, which is governed, in the $\omega\to 0^+$ limit, by low energy excitations. Low energy excitations of the system are electron-hole pair excitations in the leads and excitations in the dot configuration. But as demonstrated in Sec. II B, the excitation in the dot configuration has a *finite* excitation energy due to the avoided crossing and thus excitations in the dot can be neglected in the $\omega\to 0^+$ limit [27]. On the other hand, excitations in the leads can have infinitesimal excitation energies and thus contribute to $\mathcal{N}(E_0+\hbar\omega)$. Figure (2) shows schematically four groups of excited states $|\Psi_n\rangle$ with a single electron-hole pair excitation in the leads. States $|\Psi_n\rangle$ in groups (a) and (b) may be neglected for the density of states evaluation since $|\langle\Psi_0|\delta\hat{N}^{\rm diff}|\Psi_n\rangle|^2 = 0$ up to second order in Γ and $\varepsilon_N-\varepsilon_1$. On the other hand, for states $|\Psi_n\rangle$ in groups (c) and (d), $|\langle\Psi_0|\delta\hat{N}^{\rm diff}|\Psi_n\rangle|^2 \sim \mathcal{O}(\Gamma)^2$ and groups (c) and (d) contribute $\hbar\omega\mathcal{N}_{\rm sp}^{\rm (L)}(\epsilon_F)\mathcal{N}_{\rm sp}^{\rm (R)}(\epsilon_F)$ to $\mathcal{N}(E_0+\hbar\omega)$, where $\mathcal{N}_{\rm sp}^{\rm (L)}(\epsilon_F)$ and $\mathcal{N}_{\rm sp}^{\rm (R)}(\epsilon_F)$ are single particle densities of states of the left and right leads, respectively, at the Fermi energy. We remark that states $|\Psi_n\rangle$ with n pairs of electron-hole excitations also contribute to $\mathcal{N}(E_0+\hbar\omega)$ but their contribution scales as ω^{2n-1}, which is negligible in the $\omega\to 0^+$ limit.

Next we evaluate $\langle\Psi_0|\delta\hat{N}^{\rm diff}|\Psi_n\rangle$. Let $|\varphi_0\rangle \equiv P_1|\Psi_0\rangle$, $|\varphi_n\rangle \equiv P_1|\Psi_n\rangle$, which are solutions of $H_{\rm eff}(E_0)|\varphi_0\rangle = E_0|\varphi_0\rangle$ and $H_{\rm eff}(E_n)|\varphi_n\rangle = E_n|\varphi_n\rangle$. According to the Schrieffer-Wolff transformation, $|\Psi_0\rangle$ and $|\Psi_n\rangle$ are related to $|\varphi_0\rangle$ and $|\varphi_n\rangle$ as follows,

$$|\Psi_0\rangle = \frac{1}{E_0-H_{00}}H_{01}|\varphi_0\rangle + |\varphi_0\rangle + \frac{1}{E_0-H_{22}}H_{21}|\varphi_0\rangle, \tag{12}$$

$$|\Psi_n\rangle = \frac{1}{E_n-H_{00}}H_{01}|\varphi_n\rangle + |\varphi_n\rangle + \frac{1}{E_n-H_{22}}H_{21}|\varphi_n\rangle, \tag{13}$$

where the first, second, third terms represent the projections of $|\Psi_0\rangle$ and $|\Psi_n\rangle$ onto the subspace with zero, one, two electrons in the dot, respectively. By using Eqs. (12) and (13) and recalling that $P_s\delta\hat{N}^{\rm diff}P_t = 0$ for $s\neq t$ $(s,t=0,1,2)$, one finds

$$\begin{aligned}
&\langle\Psi_0|\delta\hat{N}^{\rm diff}|\Psi_n\rangle \\
&= \langle\varphi_0|H_{10}\frac{1}{E_0-H_{00}}\,\delta\hat{N}^{\rm diff}\frac{1}{E_n-H_{00}}H_{01}|\varphi_n\rangle \\
&\quad +\langle\varphi_0|\delta\hat{N}^{\rm diff}|\varphi_n\rangle \\
&\quad +\langle\varphi_0|H_{12}\frac{1}{E_0-H_{22}}\,\delta\hat{N}^{\rm diff}\frac{1}{E_n-H_{22}}H_{21}|\varphi_n\rangle.
\end{aligned} \tag{14}$$

Note that $\langle\Psi_0|\delta\hat{N}^{\rm diff}|\Psi_n\rangle$ is now expressed in terms of $|\varphi_0\rangle$ and $|\varphi_n\rangle$, which are eigenkets of $H_{\rm eff}$. We evaluate the three terms on the right hand side of Eq. (14) up to the first order in Γ and $\varepsilon_N-\varepsilon_1$ by performing the perturbation theory calculation for $H_{\rm eff}$. After some calculations, it can be verified that the first and third terms on the right hand side of Eq. (14) are finite in the $\omega\to 0^+$ limit while the second term is proportional to ω^{-1}. Thus in the $\omega\to 0^+$ limit, $\langle\Psi_0|\delta\hat{N}^{\rm diff}|\Psi_n\rangle$ is completely governed by the projections of $|\Psi_0\rangle$ and $|\Psi_n\rangle$ onto the subspace with one electron in the dot. Note that the ω^{-2} dependence of $\left|\langle\Psi_0|\delta\hat{N}_{\rm diff}|\Psi_n\rangle\right|^2$ is canceled by $[\mathcal{N}(E_0+\hbar\omega)\,\hbar\omega]\propto\omega^2$, producing a finite G [Eq. (11)] in the $\omega\to 0^+$ limit. Combined with the result for $\mathcal{N}(E_0+\hbar\omega)$, one obtains

$$\begin{aligned}
G &= \frac{2\pi e^2}{\hbar}\mathcal{N}_{\rm sp}^{\rm (L)}(\epsilon_F)\mathcal{N}_{\rm sp}^{\rm (R)}(\epsilon_F) \\
&\quad\times\left|-\frac{1}{-\varepsilon_{\rm ave}}A_+B_+^* + \frac{1}{\varepsilon_{\rm ave}+U_{\rm CB}}A_-B_-^*\right|^2,
\end{aligned} \tag{15}$$

where

$$\begin{aligned}
&A_+ \equiv \alpha t_1^{({\rm L})^*} + \beta t_N^{({\rm L})^*}, \quad B_+ \equiv \alpha t_1^{({\rm R})^*} + \beta t_N^{({\rm R})^*}, \\
&A_- \equiv \beta^* t_1^{({\rm L})^*} - \alpha^* t_N^{({\rm L})^*}, \quad B_- \equiv \beta^* t_1^{({\rm R})^*} - \alpha^* t_N^{({\rm R})^*}.
\end{aligned}$$

Here $\binom{\alpha}{\beta}$ and $\binom{\beta^*}{-\alpha^*}$ are the normalized eigenvectors of Eq. (10) corresponding to its lower and higher eigenvalues, respectively.

Before we discuss in the next subsection the implications of Eq. (15) regarding the transmission zero, we discuss the physical interpretation of Eq. (15) in terms of elastic cotunneling processes. For this purpose, we first introduce two linear combinations $|\mathrm{D1}\rangle$ and $|\mathrm{D2}\rangle$ of the dot states $|1\rangle$ and $|N\rangle$,

$$|\mathrm{D1}\rangle \equiv \alpha|1\rangle + \beta|N\rangle, \tag{16}$$

$$|\mathrm{D2}\rangle \equiv \beta^*|1\rangle - \alpha^*|N\rangle. \tag{17}$$

Since $\binom{\alpha}{\beta}$ and $\binom{\beta^*}{-\alpha^*}$ are the two normalized eigenvectors of Eq. (10), $|\mathrm{D1}\rangle$ and $|\mathrm{D2}\rangle$ represent two effective single-particle eigenstates in the dot. In terms of $|\mathrm{D1}\rangle$ and $|\mathrm{D2}\rangle$, Eq. (15) has a simple physical meaning; A_+ and B_+ represent effective hopping matrix elements from $|\mathrm{D1}\rangle$ to the left and right electrodes, respectively, and A_- and B_- represent effective hopping matrix elements from $|\mathrm{D2}\rangle$ to the left and right electrodes, respectively. In this description, the first term $\frac{1}{-\varepsilon_{\mathrm{ave}}}A_+B_+^*$ in Eq. (15) can be interpreted as the amplitude of the cotunneling process in Fig. 3(a); an electron in $|\mathrm{D1}\rangle$ hops to the left electrode first (A_+) and then another electron in the right electrode hops to the $|\mathrm{D1}\rangle$ (B_+^*). The energy of the intermediate virtual state with respect to the initial state is $-\varepsilon_{\mathrm{ave}}(>0)$. Similarly the second term $\frac{1}{\varepsilon_{\mathrm{ave}}+U_{\mathrm{CB}}}A_-B_-^*$ in Eq. (15) can be interpreted as the amplitude of the cotunneling process in Fig. 3(b); an electron in the right electrode hops to the empty level $|\mathrm{D2}\rangle$ (B_-^*) and then the electron in $|\mathrm{D2}\rangle$ hops to the left electrode (A_-). The energy of the intermediate virtual state with respect to the initial state is $\varepsilon_{\mathrm{ave}}+U_{\mathrm{CB}}(>0)$. Note that both cotunneling processes are elastic since the initial and final states have the same energy. To obtain the total transition amplitude, the transition amplitudes for the two elastic cotunneling processes should be summed up coherently. A careful comparison of the two final states in Fig. 3(a) and (b) indicates that they differ by a pair-wise electron exchange of the electron in $|\mathrm{D1}\rangle$ and an electron in the left lead. This pair-wise exchange gives rise to a relative phase factor (-1), which explains the $(-)$ sign in front of $\frac{1}{-\varepsilon_{\mathrm{ave}}}A_+B_+^*$ in Eq. (15). In this description in terms of the effective dot states $|\mathrm{D1}\rangle$ and $|\mathrm{D2}\rangle$, Eq. (15) is also consistent with the (second order) golden rule formula,

$$w_{[i]\to[f]} = \frac{2\pi}{\hbar}\overline{\left|\sum_m \frac{\tilde{H}_{fm}\tilde{H}_{mi}}{E_i - E_f}\right|^2}\,\rho\left(E_f\right)|_{E_f\simeq E_i} \tag{18}$$

where the effective perturbation $\tilde{H}$ represents the hopping between the leads and the effective dot states $|\mathrm{D1}\rangle$ and $|\mathrm{D2}\rangle$, and $w_{[i]\to[f]}$ is related to G via $ew_{[i]\to[f]} = G\Delta V$ and $\rho\left(E_f\right)|_{E_f\simeq E_i} = e\Delta V\mathcal{N}_{\mathrm{sp}}^{(\mathrm{L})}(\epsilon_F)\mathcal{N}_{\mathrm{sp}}^{(\mathrm{R})}(\epsilon_F)$. Here ΔV denotes the voltage difference between the two leads.

D. Transmission zero

We examine in this subsection the $\varepsilon_{\mathrm{ave}}$-dependence of G and demonstrate the appearance of the transmission zero. Experimentally, $\varepsilon_{\mathrm{ave}}$ can be modulated by the gate voltage applied to the dot [Eq. (6)]. To get an insight, we first examine a special case of symmetric hopping with $t_1^{(\mathrm{L})} = t_1^{(\mathrm{R})} = t_1$ and $t_N^{(\mathrm{L})} = t_N^{(\mathrm{R})} = t_N$. In this case, both $A_+B_+^*$ and $A_-B_-^*$ are real and thus the total amplitude (within $|\cdots|$) in Eq. (15) is real. Based on behaviors of α and β in terms of $\varepsilon_{\mathrm{ave}}$, which was reviewed in Sec. II B, one can estimate the conductance in the following two regions, (1) $-1 \lesssim \frac{\varepsilon_{\mathrm{ave}}}{U_{\mathrm{CB}}} \lesssim -\frac{1}{2}$ and (2) $-\frac{1}{2} \lesssim \frac{\varepsilon_{\mathrm{ave}}}{U_{\mathrm{CB}}} \lesssim 0$. In case (1), $\alpha \simeq 1$ and $\beta \simeq 0$, and the total amplitude of the two cotunneling processes in Eq. (15) becomes

$$\frac{|t_1|^2}{\varepsilon_{\mathrm{ave}}} + \frac{|t_N|^2}{\varepsilon_{\mathrm{ave}} + U_{\mathrm{CB}}}, \tag{19}$$

which is a positive real number as shown in Fig. 4. In case (2), $\alpha \simeq 0$ and $\beta \simeq 1$, and the total amplitude in the region (2) reduces similarly to

$$\frac{|t_N|^2}{\varepsilon_{\mathrm{ave}}} + \frac{|t_1|^2}{\varepsilon_{\mathrm{ave}} + U_{\mathrm{CB}}}, \tag{20}$$

which is a negative real number as shown in Fig. 4. Since the total amplitude varies continuously and remains real in the whole range $-1 \lesssim \frac{\varepsilon_{\mathrm{ave}}}{U_{\mathrm{CB}}} \lesssim 0$, Eqs. (19) and (20) indicate that the total amplitude should vanish identically at a particular value of $\varepsilon_{\mathrm{ave}}$ near $\frac{\varepsilon_{\mathrm{ave}}}{U_{\mathrm{CB}}} = -\frac{1}{2}$, and the transmission zero appears. Note that the transmission zero appears in the region where the ground state dot configuration changes.

Next we examine a generic situation with non-symmetric hopping and demonstrate that the transmission zero persists even in this situation if the system has a time reversal symmetry. In a time-reversal symmetric system, all hopping matrix elements $t_1^{(\mathrm{L})}$, $t_1^{(\mathrm{R})}$, $t_N^{(\mathrm{L})}$, $t_N^{(\mathrm{R})}$ can be taken real upon proper gauge transformations of the electron annihilation operators, $a \to e^{i\theta_a}a$, $b \to e^{i\theta_b}b$, $c \to e^{i\theta_c}c$. Then Eq. (10) becomes a real symmetric matrix, and both α and β and also $A_+B_+^*$, $A_-B_-^*$ become real. Hence the total amplitude [expression within the absolute value symbol in Eq. (15)] again becomes real and it can be verified that the amplitude changes its sign

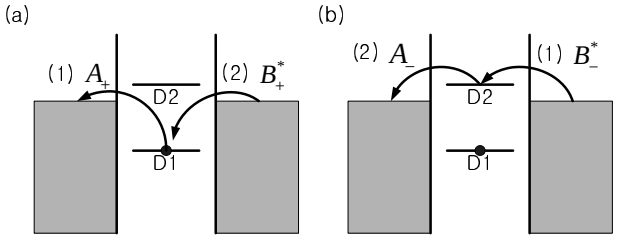

FIG. 3: Two elastic cotunneling processes of two electrons. (a) and (b) describe hopping via the effective dot states $|\mathrm{D1}\rangle$ and $|\mathrm{D2}\rangle$, respectively. The arrows indicate the electron hopping direction. The number (1) and (2) above the arrows is to denote which hopping occurs first (1) or next (2). Associated hopping amplitudes are also denoted.

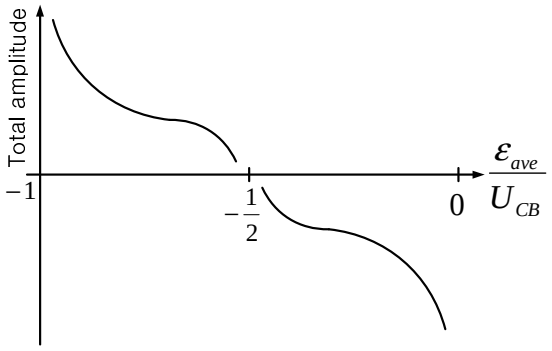

FIG. 4: Schematic plot of the transmission amplitude in two regions: (1) $-1 \lesssim \frac{\varepsilon_{\rm ave}}{U_{\rm CB}} \lesssim -\frac{1}{2}$ and (2) $-\frac{1}{2} \lesssim \frac{\varepsilon_{\rm ave}}{U_{\rm CB}} \lesssim 0$. The regime around $\frac{\varepsilon_{\rm ave}}{U_{\rm CB}} \sim -\frac{1}{2}$ requires a numerical evaluation [see Figs. 1(b) and 5].

similarly to Fig. 4, signaling the occurrence of the transmission zero. Figure 1(b) shows numerical calculation of conductance for a time-reversal symmetric system in the dot configuration crossover regime $\varepsilon_{\rm ave}/U_{\rm CB} \sim -1/2$. Note that the transmission zero happens indeed when the configuration change occurs. We have assigned coupling coefficients as follows: $t_1^{(\rm L)}/t_1^{(\rm R)} = 1, t_N^{(\rm L)}/t_1^{(\rm R)} = 10, t_N^{(\rm R)}/t_1^{(\rm R)} = 11$.

Next we consider systems without the time-reversal symmetry. Then not all hopping matrix elements can be taken real, and the phases of $t_i^{(j)}$ do affect G. From Eqs. (10) and (15), it can be verified that the phase dependence of G occurs only via the total phase of $t_1^{(\rm L)} t_N^{(\rm L)*} t_N^{(\rm R)} t_1^{(\rm R)*}$ instead of individual phases. Figure 5 shows the G vs. $\varepsilon_{\rm ave}/U_{\rm CB}$ graphs as a function of the total phase. Note that the transmission zero appears only when $t_1^{(\rm L)} t_N^{(\rm L)*} t_N^{(\rm R)} t_1^{(\rm R)*}$ is real (total phase of 0, π, or 2π), and the transmission zero is replaced by a small but finite conductance dip when $t_1^{(\rm L)} t_N^{(\rm L)*} t_N^{(\rm R)} t_1^{(\rm R)*}$ is *not* real. When $t_1^{(\rm L)} t_N^{(\rm L)*} t_N^{(\rm R)} t_1^{(\rm R)*}$ is real, the all $t_i^{(j)}$'s can be taken real via proper gauge transformations of the electron annihilation operators, implying that the system has the time-reversal symmetry. Thus this total phase dependence of the transmission zero illustrates the role of the time-reversal symmetry for the transmission zero. This result is consistent with the analysis [8] based on the Friedel sum rule and also agrees with the result [28] for the Fano-resonance-based theory.

E. Transmission phase

Here we consider the phase of the transmission amplitude through the quantum dot. Experimentally testable definition of the transmission phase requires an interference configuration such as the Aharonov-Bohm ring used in Ref. [2]. For this purpose, we introduce a direct hopping channel from the left to right leads, not mediated

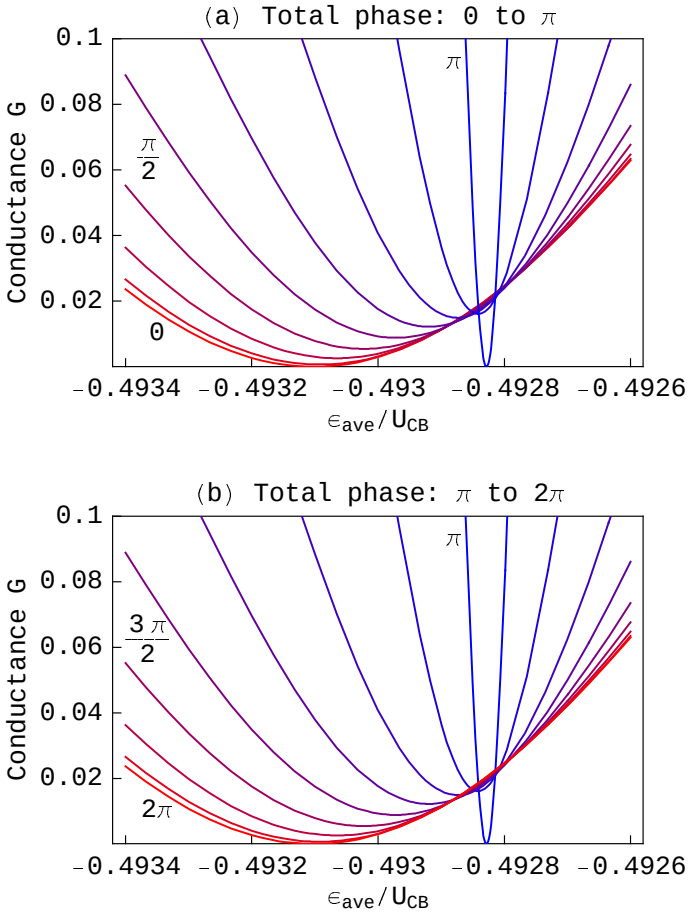

FIG. 5: (Color online) Evolution of the conductance vs. $\varepsilon_{\rm ave}/U_{\rm CB}$ curve as a function of the total phase of $t_1^{(\rm L)} t_N^{(\rm L)*} t_N^{(\rm R)} t_1^{(\rm R)*}$. (a) From the total phase of 0 (red, labeled as 0) to π (blue, labeled as π) in steps of $\pi/8$ and (b) from π (blue, labeled as π) to 2π (red, labeled as 2π) in steps of $\pi/8$. The transmission zero occurs only when the total phase is 0, π, or 2π. Note that the horizontal axis is magnified considerably compared to that of Fig. 1(b), so that the whole span of the horizontal axis in these figures covers a narrow portion of the $\varepsilon_{\rm ave}/U_{\rm CB}$ range near the conductance dip in Fig. 1(b). The units for the conductance in (a) and (b) are the same as that used in Fig. 1(b).

by the dot levels. Equation (15) is then modified to

$$G = \frac{2\pi e^2}{\hbar} \mathcal{N}_{\rm sp}^{(\rm L)}(\epsilon_F) \mathcal{N}_{\rm sp}^{(\rm R)}(\epsilon_F) \times \left| -\frac{1}{-\varepsilon_{\rm ave}} A_+ B_+^* + \frac{1}{\varepsilon_{\rm ave} + U_{\rm CB}} A_- B_-^* + t^{(\rm R)\to(\rm L)} \right|^2, \tag{21}$$

where $t^{(\rm R)\to(\rm L)}$ is the transmission amplitude of the direct hopping from the left to right leads. Thus the phase of the transmission amplitude *through* a quantum dot is nothing but the phase of $\frac{1}{\varepsilon_{\rm ave}} A_+ B_+^* + \frac{1}{\varepsilon_{\rm ave}+U_{\rm CB}} A_- B_-^*$. Figure 6 shows the transmission phase

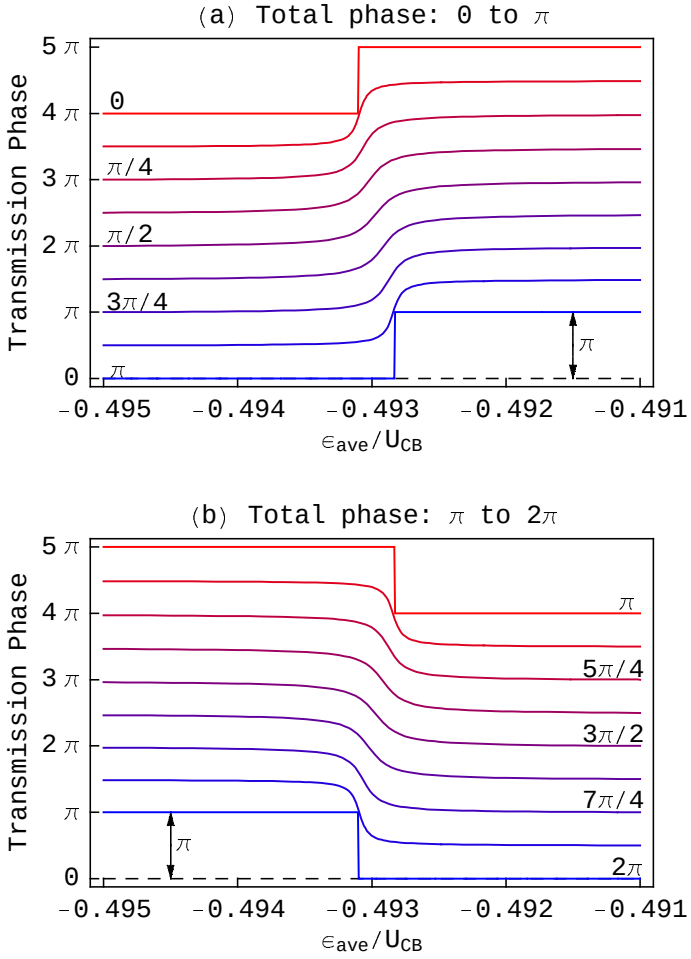

FIG. 6: (Color online) The transmission phase vs $\varepsilon_{\rm ave}/U_{\rm CB}$ as a function of the total phase of $t_1^{(\rm L)}t_N^{(\rm L)*}t_N^{(\rm R)}t_1^{(\rm R)*}$. (a) From the total phase 0 (red line, labeled as 0) to π (blue line, labeled as π) and (b) from π (red line, labeled as π) to 2π (blue line, labeled as 2π). For clarity, the curves are shifted vertically by proper amounts.

versus $\varepsilon_{\rm ave}/U_{\rm CB}$ graphs as a function of the total phase of $t_1^{(\rm L)}t_N^{(\rm L)*}t_N^{(\rm R)}t_1^{(\rm R)*}$. In systems with time-reversal symmetry (with the total phase 0, π, or 2π), the transmission phase changes abruptly by π at transmission zero even though the dot configuration of the ground state changes smoothly. In systems without time-reversal symmetry, the transmission phase changes smoothly by π. Note that when the total phase is between π and 2π, the transmission phase drops by π as $\varepsilon_{\rm ave}/U_{\rm CB}$ is increased, and when the total phase is between 0 and π, it rises by π.

III. CONCLUSION AND DISCUSSION

In the interaction-based theory [12] of the experimental results in Ref. [2], the dot configuration change in conductance valleys is responsible for the sudden phase drop. We performed the perturbative conductance calculation up to the first nonvanishing order in the electron hopping matrix elements (fourth order in $t_i^{(j)}$) and found that the dot configuration change is accompanied by the transmission zero. According to the Friedel sum rule, transmission zero is a mandatory feature for the sudden phase drop in a spinless time-reversal symmetric one-dimensional systems [8], and our calculation shows that the interaction-based theory [12] is consistent with the prediction of the Friedel sum rule (at least up to the fourth order in $t_i^{(j)}$).

A few remarks are in order. We first compare the interaction-based theory [12] and the Fano-resonance-based theory [9, 10, 11] of the sudden phase drop and the in-phase resonance. The two theories are similar in the sense that they both assume the coexistence of strongly coupled levels and weakly coupled levels. But regarding the roles of electron-electron interaction, the two theories are different; While the interaction is essentially ignored in the Fano-resonance-based theory [9, 10, 11], it plays a crucial role in the interaction-based theory [12]. One manifestation of this difference is the relevance or irrelevance of the signs of the hopping matrix elements. For simplicity of illustration, we assume a time-reversal symmetric system, where all hopping matrix elements may be assumed to be real. According to Ref. [29], which addresses the role of the hopping matrix signs in the context of the Fano-resonance-based theory, the sudden phase drop (and also transmission zero) may or may not appear between two consecutive Coulomb blockade resonance peaks, depending on the relative signs of the hopping matrix elements. In the interaction-based theory, in contrast, the signs of the hopping matrix elements are largely irrelevant to the existence of the sudden phase drop (and also transmission zero). As demonstrated in Figs. 5 and 6, the sudden phase drop (and transmission zero) persists even when the sign of one of $t_i^{(j)}$'s changes (and thus the total phase of $t_1^{(\rm L)}t_N^{(\rm L)*}t_N^{(\rm R)}t_1^{(\rm R)*}$ is altered from 0 to π or from π to 0). Only its position is shifted by a small amount ($\delta\varepsilon_{\rm ave}/U_{\rm CB} \ll 1$) due to the sign change.

Our discussion so far neglected the spin degrees of freedom. When the transport is spin-dependent or when spin-flip scattering becomes possible, it is crucial to take into account the spin degrees of freedom. In this case, the electron transmission from one electrode to the other is described by four (instead of one) transmission amplitudes, $t_{\uparrow\uparrow}$, $t_{\downarrow\downarrow}$, $t_{\uparrow\downarrow}$, $t_{\downarrow\uparrow}$, and each transmission amplitude may have different gate voltage dependence. Reference [23] addressed spin effects of the interaction-based theory. In the limit $t_1^{(\rm R/L)} \ll t_N^{(\rm R/L)}$, the total conductance ($\propto |t_{\uparrow\uparrow}|^2 + |t_{\downarrow\downarrow}|^2 + |t_{\uparrow\downarrow}|^2 + |t_{\downarrow\uparrow}|^2$) shows interesting features (see Fig. 3 in Ref. [23]) near the gate voltage for the dot configuration change. Unfortunately the individual behaviors of the four amplitudes are not addressed. Further insights into the experimental results in Ref. [2] may be obtained from spin resolved studies of the transmission amplitudes and their dependence on

time-reversal symmetry.

Acknowledgments

This work was supported by the SRC/ERC program (Grant No. R11-2000-071) and the Basis Research Program (Grant No. R01-2005-000-10352-0) of MOST/KOSEF, by the POSTECH Core Research Program, and by the Korea Research Foundation Grant (Grant No. KRF-2005-070-C00055 and BK21 program) funded by the Korean Government (MOEHRD).

APPENDIX A: LINEAR RESPONSE

To obtain the linear response conductance of the system described by the Hamiltonian H, we first introduce the voltage bias into the total Hamiltonian,

$$H_{\rm bias} = \sum_k \frac{e\Delta V}{2}\; a_k^\dagger a_k - \sum_l \frac{e\Delta V}{2}\; b_l^\dagger b_l, \qquad \text{(A1)}$$

and use the method of the adiabatic turning on,

$$H_{\rm tot}(t) = H + F(t) H_{\rm bias},$$

where $F(t) = e^{\eta t}\cos\omega t$ with $\eta \to 0^+$ and the limit $\omega \to 0^+$ will be taken to obtain the DC conductance [30]. From the Kubo formula [31], the current expectation value $\overline{I}(t)$ in the linear response regime is readily obtained as follows:

$$\begin{aligned}\overline{I}(t) \;=\; & \lim_{\eta\to 0^+} \frac{1}{i\hbar}\int_{-\infty}^{t} dt' F(t') \\ & \times \langle\Psi_0|\left[e^{\frac{i}{\hbar}(t-t')H}\hat{I}e^{-\frac{i}{\hbar}(t-t')H}, H_{\rm bias}\right]|\Psi_0\rangle,\end{aligned} \qquad \text{(A2)}$$

where $|\Psi_0\rangle$ is the exact ground state of H and $\hat{I}$ is the current operator given by

$$\hat{I} = \frac{d}{dt}\left(\frac{\hat{Q}^{(\rm R)} - \hat{Q}^{(\rm L)}}{2}\right) = \frac{e}{2i\hbar}\left[H, \hat{N}^{(\rm R)} - \hat{N}^{(\rm L)}\right]. \qquad \text{(A3)}$$

Here $\hat{N}^{(\rm L)} \equiv \sum_k a_k^\dagger a_k$ ($\hat{N}^{(\rm R)} \equiv \sum_k b_k^\dagger b_k$) counts the number of electrons in the left (right) lead, and $\hat{Q}^{(\rm L)} \equiv -e\hat{N}^{(\rm L)}$, $\hat{Q}^{(\rm R)} \equiv -e\hat{N}^{(\rm R)}$. After inserting the closure $\sum_{n=0}|\Psi_n\rangle\langle\Psi_n|$ into the above expression, where $|\Psi_n\rangle$ is the n-th excited states of H with energy E_n, one performs the integration over time t and take $\eta \to 0^+$ limit to obtain the expression for the conductance G,

$$\begin{aligned} G =& \frac{\overline{I}(0)}{\Delta V} \\ =& \lim_{\omega\to 0^+} \frac{\pi e^2}{4\hbar}\sum_n \delta\left(E_n - E_0 - \hbar\omega\right)\hbar\omega |\langle\Psi_0|\hat{N}^{\rm diff}|\Psi_n\rangle|^2, \end{aligned} \qquad \text{(A4)}$$

where $\hat{N}^{\rm diff} \equiv \hat{N}^{(\rm L)} - \hat{N}^{(\rm R)}$. We use the identity $\langle\Psi_0|\hat{N}^{\rm diff}|\Psi_n\rangle = \langle\Psi_0|\delta\hat{N}^{\rm diff}|\Psi_n\rangle$ where $\delta\hat{N}^{\rm diff} \equiv \hat{N}^{\rm diff} - \langle\Psi_0|\hat{N}^{\rm diff}|\Psi_0\rangle$ and obtain the final expression,

$$G = \frac{\pi e^2}{4\hbar}\lim_{\omega\to 0^+}\left[\mathcal{N}\left(E_0+\hbar\omega\right)\hbar\omega\right]\overline{\left|\langle\Psi_0|\delta\hat{N}^{\rm diff}|\Psi_n\rangle\right|^2}_{E_n = E_0+\hbar\omega}, \qquad \text{(A5)}$$

where $\mathcal{N}(E)$ is the many-body density of states and $\overline{\left|\langle\Psi_0|\delta\hat{N}^{\rm diff}|\Psi_n\rangle\right|^2}_{E_n=E_0+\hbar\omega}$ represents the average of $\left|\langle\Psi_0|\delta\hat{N}^{\rm diff}|\Psi_n\rangle\right|^2_{E_n=E_0+\hbar\omega}$ over states with $E_n = E_0 + \hbar\omega$.

[1] A. Yacoby, M. Heiblum, D. Mahalu, and H. Shtrikman, Phys. Rev. Lett. **74**, 4047(1995).
[2] E. Schuster, E. Buks, M. Heiblum, D. Mahalu, V. Umansky, and Hadas Shtrikman, Nature (London) **385**, 417(1997).
[3] G. Breit and E. Wigner, Phys. Rev. **49**, 519 (1936).
[4] M. Sigrist, A. Fuhrer, T. Ihn, K. Ensslin, S. E. Ulloa, W. Wegscheider, and M. Bichler, Phys. Rev. Lett. **93**, 066802 (2004).
[5] M. Avinun-Kalish, M. Heiblum, O. Zarchin, D. Mahalu, and V. Umansky, Nature **436**, 529 (2005).
[6] For a review, see for example G. Hackenbroich, Phys. Rep. **343**, 463 (2001).
[7] G. Hackenbroich and H. A. Weidenmüller, Phys. Rev. Lett. **76**, 110 (1996); Y. Oreg and Y. Gefen, Phys. Rev. B **55**, 13726 (1997); G. Hackenbroich, W. D. Heiss, and H. A. Weidenmüller, Phys. Rev. Lett. **79**, 127 (1997); R. Baltin, Y. Gefen, G. Hackenbroich, and H. A. Weidenmuller, Eur. Phys. J. B **10**, 119 (1999); R. Baltin and Y. Gefen, Phys. Rev. Lett. **83**, 5094 (1999); A. Levy Yeyati and M. Büttiker, Phys. Rev. B **62**, 7307 (2000); H. A. Weidenmüller, Phys. Rev. B **65**, 245322 (2002); A. Aharony, O. Entin-Wohlman, B. I. Halperin, and Y. Imry, Phys. Rev. B **66**, 115311 (2002).
[8] H.-W. Lee, Phys. Rev. Lett. **82**, 2358(1999).
[9] H. Q. Xu and W. Sheng, Phys. Rev. B **57**, 11903 (1998).
[10] P. S. Deo and A. M. Jayannavar, Mod. Phys. Lett. B **10**, 787 (1996); P. S. Deo, Solid State Commun. **107**, 69 (1998).
[11] C.-M. Ryu and S. Cho, Phys. Rev. B **58**, 3572 (1998).
[12] P. G. Silvestrov and Y. Imry, Phys. Rev. Lett. **85**, 2565 (2000).
[13] J. S. Langer and V. Ambegaokar, Phys. Rev. **121**, 1090 (1961).
[14] U. Fano, Phys. Rev. **124**, 1866 (1961).
[15] O. Entin-Wohlman, A. Aharony, Y. Imry, and Y. Levin-

son, J. Low Temp. Phys. **126**, 1251 (2002).
[16] T. Nakanishi, K. Terakura, and T. Ando, Phys. Rev. B **69**, 115307 (2004).
[17] K. Kobayashi, H. Aikawa, S. Katsumoto, and Y. Iye, Phys. Rev. Lett. **88**, 256806 (2002); Phys. Rev. B **68**, 235304 (2003).
[18] When the spin degrees of freedom are taken into account, the scattering matrix **S** should be expanded to a 4×4 matrix.
[19] T. Taniguchi and M. Büttiker, Phys. Rev. B **60**, 13814 (1999).
[20] P. G. Silvestrov and Y. Imry [Phys. Rev. Lett. **90**, 106602 (2003)] found via a different analysis that the phase drop has to be always sudden in a time reversal symmetric system.
[21] H.-W. Lee and C. S. Kim, Phys. Rev. B **63**, 075306 (2001).
[22] Coexistence of broad and narrow levels is experimentally supported in an experiment by H. Aikawa, K. Kobayashi, A. Sano, S. Katsumoto, and Y. Iye [J. Phys. Soc. Jpn **73**, 3235 (2004)].
[23] P. G. Silvestrov and Y. Imry, Phys. Rev. B **65**, 035309 (2002).
[24] The application of the Friedel sum to an interacting system is valid as long as the system remains as a Fermi liquid. For a more mathematical statement of this condition, see Ref. [13].
[25] See, for instance, A. C. Hewson, *The Kondo Problem to Heavy Fermions* (Cambridge University Press, New York, 1993).
[26] When the procedure in Sec. II A and II B is applied to the model Hamiltonian addressed in Ref. [23], which takes into account the spin degrees of freedom as well, it reproduces the matrix elements Eq. (15) in Ref. [23] once the diagonal elements H_{11} and H_{22} are subtracted by a proper constant.
[27] Calculation of the current expectation value involves various limiting procedures; (1) $\delta_{\rm sp} \to 0$ where $\delta_{\rm sp}$ is the single-particle level spacing in the leads, (2) $\eta \to 0+$, (3) $\omega \to 0+$, (4) $H' \to 0$. For correct evaluation, these four limiting procedures should be taken in the following order, (1) → (2) → (3) → (4). The reversal of the order, for example (3) and (4), may result in a wrong expression for the current expectation value.
[28] T.-S. Kim, S. Y. Cho, C. K. Kim, and C.-M. Ryu, Phys. Rev. B **65**, 245307 (2002).
[29] A. Silva, Y. Oreg, and Y. Gefen, Phys. Rev. B **66**, 195316 (2002); T.-S. Kim and S. Hershfield, Phys. Rev. B **67**, 235330 (2003).
[30] E. N. Economou and C. M. Soukoulis, Phys. Rev. Lett. **46**, 618(1981); D. S. Fisher and P. A. Lee, Phys. Rev. B **23**, 6851(1981).
[31] See Appendix B in Ref. [25] or O. Madelung, *Introduction to Solid-State Theory* (Springer-Verlag, Berlin, 1981), p. 365.